17th World Conference on Earthquake Engineering, 17WCEE
Sendai, Japan - September 13th to 18th 2020

STUDY ON THE PARAMETERS OF THE HYPERBOLIC MODEL UNER PORE PRESSURE INCREASE

Rui Sun [(1)], Wei Zhang[(2)] ,Xiaofei Li[(3)]

[(1)] *Professor, Institution of Engineering Mechanics, China Earthquake Administration, Key Laboratory of Earthquake Engineering and Engineering Vibration of China Earthquake Administration, Harbin, China, iemsr@163.com*
[(2)] *Master's degree candidate, Institution of Engineering Mechanics, China Earthquake Administration, Key Laboratory of Earthquake Engineering and Engineering Vibration of China Earthquake Administration, Harbin, China, 13477071564@163.com*
[(3)] *Lecturer, Binzhou University , Binzhou, China, lxf2011iem@126.com*

Abstract

The key to describing the dynamic constitutive relation of liquefiable soil layer with the hyperbolic model is to provide the cyclic maximum shear modulus and cyclic ultimate shear stress of sandy soil under the application of cyclic loading. Focusing on several types of sandy soils with different relative densities, we conducted liquefaction testing under the conditions of different equal cyclic stresses and equal consolidation using a new type of high-precision dynamic three-axis instrument. We investigated the influence modes and patterns of pore water pressure on the cyclic maximum shear modulus and cyclic ultimate shear stress of saturated sandy soil, and proposed the calculation equations with different precision requirements for the cyclic maximum shear modulus and cyclic ultimate shear stress of sandy soil with consideration of pore pressure increase. The results showed that the increase of pore pressure had a significant impact on the cyclic maximum shear modulus and cyclic ultimate shear stress of saturated sandy soil. Moreover, the cyclic maximum shear modulus ratio and the cyclic ultimate shear stress decreased with the increase of pore pressure ratio. The relationship between the cyclic maximum shear modulus and pore pressure ratio for sandy soil under the condition of pore pressure increase can be expressed as a unified linear relation that is independent of sand type and relative density, and the pore pressure ratio is equal to the relative reduction of the cyclic maximum shear modulus. The relationship between the cyclic ultimate shear stress and pore pressure ratio under pore pressure increase can be expressed as quadratic curve related to sand type and relative density with the consideration of more accurate requirement. It can also be simplified as a unified linear relation independent of sand type and relative density, and in this case the pore pressure ratio was equal to the relative reduction of the cyclic ultimate shear stress. The cyclic maximum shear modulus of sandy soil under pore pressure increase did not follow the equation of Hardin initial maximum shear modulus. Therefore, the cyclic maximum shear modulus during the liquefaction process would be overestimated using the Hardin equation; in particular, in the sensitive range (0.6 to 0.8 of pore pressure ratio), the cyclic maximum shear modulus could be overestimated about 80% to 140%.

Keywords: liquefaction, hyperbolic model, cyclic maximum shear modulus, pore pressure increase

1. Introduction

The hyperbolic model[1] is a widely used elastic-plastic dynamic constitutive model for soil. Two mechanical parameters are needed for hyperbolic model to describe the hysteresis curves of soils under the application of cyclic loading: the (initial) the maximum shear modulus, $G_{max,0}$, and the (initial) ultimate shear stress, $\tau_{ult,0}$. The $G_{max,0}$ can be calculated using the Hardin equation [2] and $\tau_{ult,0}$ can be obtained by converting the cohesion and friction angle. For non-liquefied soil, the subsequent curve follows the Massing criterion under the application of cyclic loading, and its model can be still determined by these two parameters, i.e. the subsequent constitutive model assumes that $G_{max,0}$ and $\tau_{ult,0}$ are the given values, and do not vary with the application of loading and the non-linear development of soil.

However, with the increase of pore water pressure, softening behavior is observed in liquefiable soil, which is considerably different from the normal non-linear behavior of soil. With the gradual increase of cyclic loading, the pore pressure has some development. During this process in liquefiable soil, the initial

maximum tangent modulus and the initial ultimate shear modulus in the hyperbolic model are theoretically different from the non-linear liquefied soil. In this paper, the cyclic maximum shear modulus and the cyclic ultimate shear stress are referred to as $G_{max,N}$ and $\tau_{ult,N}$, respectively. These two parameters are the key to describing the stress-strain relationship of liquefiable soil using the hyperbolic model.

The Hardin equation is typically used in previous research efforts to calculate $G_{max,N}$ under varying pore pressure conditions. Matasovic and Vucetic[3] investigated the change of $G_{max,N}$ under the increase of pore pressure using a direct shear instrument. They assumed that the tangent modulus $G_{max,0}$ at the initial origin and the tangent modulus $G_{max,N}$ at the origin for subsequent hysteresis loop frame curve met the requirements of the Hardin equation. Based on this assumption, they provided the correlation expression of the cyclic maximum shear stress and pore pressure ratio, but they did not provide the correlation of the cyclic $\tau_{ult,N}$ and pore pressure, but treated the shear stress at the turning point of loading and unloading, i.e. the shear stress corresponding to the maximum strain at a certain cycle, as the ultimate shear stress for that cyclic frame curve; but in fact, there is an essential difference between them. In addition, Dobry and Ladd [4] studied the relationship between pore pressure ratio and secant shear modulus through cyclic three axial experiments. Their research indicated that the secant modulus ratio of the subsequent cycle to the first cycle correlated exponentially with effective stress, and the exponent varied between 0.4 to 0.7.

Using a new type of high-precision three axis instrument, we investigated the variation modes and patterns of the cyclic $G_{max,N}$ and cyclic $\tau_{ult,N}$ under conditions of varying pore water pressure. The purpose of this research was to determine the calculation equations for the cyclic $G_{max,N}$ and cyclic $\tau_{ult,N}$ under the increase of pore pressure in accordance with engineering practice so as to provide a basis for dynamic stress analysis of sites with consideration of liquefaction.

2. Dynamic Three-axis Experimental

2.1 Experimental Design

This research conducted liquefaction testing under different dynamic stresses using specimens of different sandy soils with different relative densities. The objective of the experiments was to investigate the pattern by which the pore water pressure affects the cyclic $G_{max,N}$ and cyclic $\tau_{ult,N}$.

The Yingkou sand was obtained from the site, which was liquefied during the 1957 Haichen Earthquake. Four soil specimens were taken from three bores with varying physical properties as shown in Table 1. All soil specimens applied in the testing procedure had identical dimensions of Φ50 mm × 100 mm. The effective consolidation confining pressure was consistently 100 kPa, and the consolidation ratio was 1.0. The experiments were carried out according to stress control mode and equal sine wave loading with a loading frequency of 1 Hz.

The relative densities of the four soil specimens for Yingkou sand were determined by the in-situ standard penetration test. The experiments utilized three amplitudes for Yingkou sand. Therefore, a total of 12 groups of liquefaction testing were conducted.

2.2 Experimental Procedures

The entire testing process included four steps: specimen loading, saturation, consolidation and vibrating liquefaction.According to the relative density, the soil specimens were saturated after compaction by layers and specimen-loading. When the measured B was greater than and equal to 0.98, the soil specimens were regarded to have reached the saturation requirement. An effective consolidation confining pressure of 100 kPa was then applied to the soil specimens. After the consolidation stabilized, the saturated specimens were loaded through the GDSLAB dynamic testing module. The variation of pore pressure was monitored in real time during loading. When pore water pressure reached the effective confining pressure, the soil specimens were assumed to be liquefied and the testing was stopped. If the pore pressure did not reach the effective confining pressure, then the dynamic stress loading was stopped after applying 1,000 cycles.

Table 1 Physical properties index of Yingkou Sand

Soil Specimen No.	Soil type	Maximum dry density (g/cm^3)	Minimum dry density (g/cm^3)	Penetration number	Relative density of specimens (%)	Dry density of specimen (g/cm^3)
ZK2-1	Silty sand	1.53	1.21	5.0	30	1.287
ZK4-2	Silty sand	1.51	1.11	16.0	50	1.282
ZK6-1	Silty sand	1.50	1.12	7.0	30	1.214
ZK6-2	Silty sand	1.54	1.14	10.0	30	1.236

3. Experimental Results and Analysis

3.1 Data Processing and Analysis Method

Figure 1 shows the schematic of an ideal stress-strain hysteresis loop, which can represent the general status of the shear stress–shear strain hysteresis curve due to cyclic loading application. The trunk equation (Eq. 1) of the hyperbolic model was used to fit the top half loop of each hysteresis loop, and thus to determine the cyclic $G_{max,N}$ and $\tau_{ult,N}$:

$$\tau = \frac{\gamma}{a+b\gamma} \tag{1}$$

where, τ is the dynamic shear stress; γ is the dynamic shear strain; a and b are experimental parameters; $G_{max,N}=1/a$ is the cyclic maximum shear modulus; and $\tau_{ult,N}=1/b$ is the cyclic ultimate shear stress.
Figure 1 provides the schematic diagram for several parameters, in which $G_{max,0}$ and $\tau_{ult,0}$ are the initial maximum shear modulus and the initial maximum ultimate shear stress, respectively; $G_{max,N}$ and $G_{max,N-1}$ correspond to the cyclic maximum shear modulus for the Nth and (N-1)th cycles, respectively; $\tau_{ult,N}$ and $\tau_{ult,N-1}$ corresponds to the cyclic ultimate shear stress for the Nth and (N-1)th cycles, respectively.

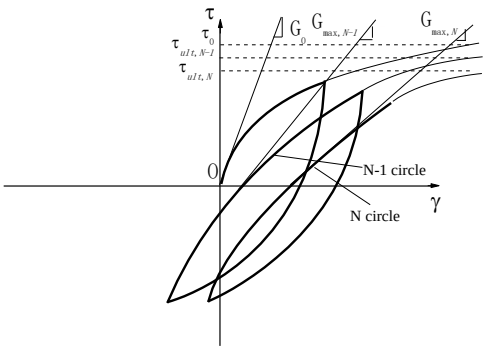

Fig. 1 Sketch of dynamic shear modulus and ultimate shear strength

3.2 Cyclic $G_{max,N}$ Under Pore Pressure Increase and Its Fitted Equation

The cyclic $G_{max,N}$ achieved from testing was normalized to obtain the varying relationship of the cyclic maximum shear modulus ratio of $G_{max,N}/G_{max,0}$ with pore water pressure ratio (Figure 2).

Figure 2 indicates that the experimental points are approximated by a straight line; therefore, the relationship between the cyclic maximum shear modulus ratio of $G_{max,N}/G_{max,0}$ and pore water pressure ratio can be expressed as

$$G_{\max,N} / G_{\max,0} = A_1 U_N + B_1 \quad (2)$$

where A_1 and B_1 are coefficients to be determined; and U_N represents the pore pressure ratio after cyclic application of current stress. The fitting parameters and correlation coefficient, R^2, determined by Equation (2) are presented in Table 2.

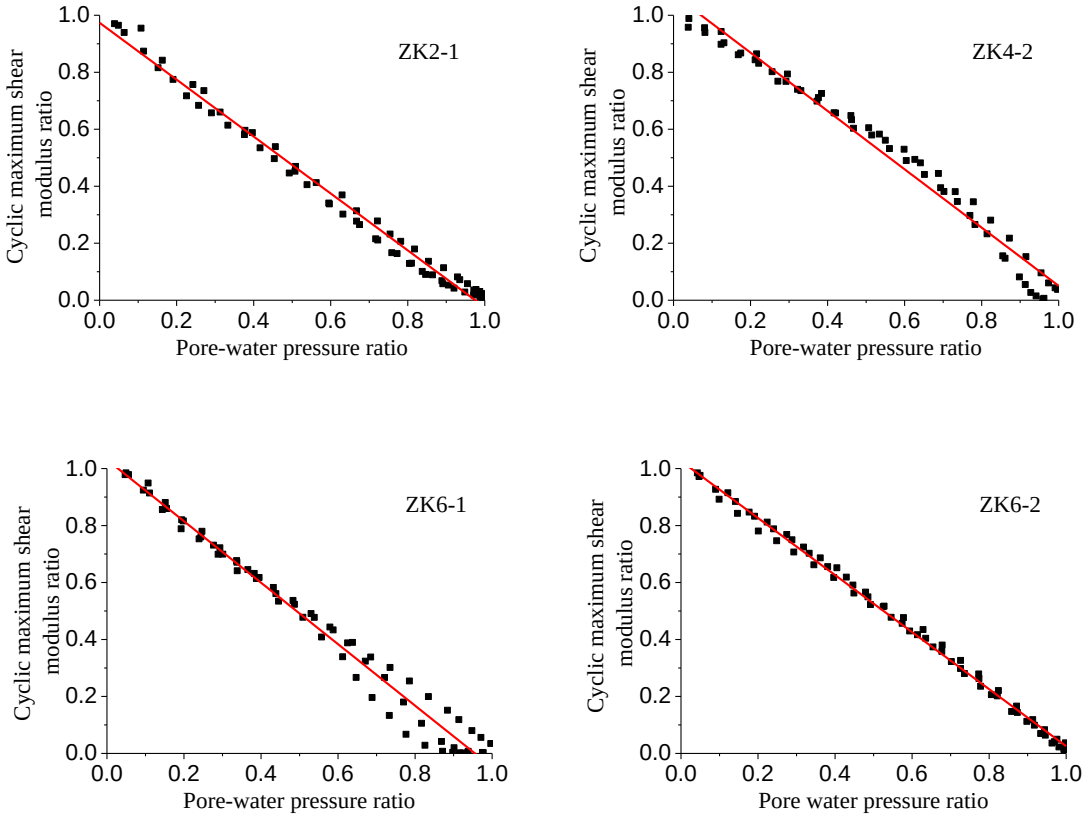

Fig. 2 Linear regressions of cyclic maximum shear modulus ratios with respect to pore-water pressure ratios

Figure 2 shows that the cyclic maximum shear modulus ratio, $G_{max,N}/G_{max,0}$, decreases approximately linearly with the increase of pore pressure ratio, and when the soil is completely liquefied, $G_{max,N}/G_{max,0}$ is close to zero. The variation of $G_{max,N}/G_{max,0}$ versus pore pressure ratio for Yingkou sand followed the same trend, which was also apparent under various compactness conditions. This suggests that the impacts relative density on the variation of $G_{max,N}/G_{max,0}$ versus pore pressure ratio can be neglected.

Table 2 Regression parameters of variation curves for cyclic maximum shear modulus versus pore pressure ratio

No.	A_1	B_1	Correlation coefficient, R^2
ZK2-1	−1.00	0.97	0.989
ZK4-2	−1.02	1.07	0.978
ZK6-1	−1.08	1.03	0.980
ZK6-2	−1.00	1.03	0.996

Table 2 indicates that the R^2 values were greater than 0.978, indicating a sound correlation. In addition, for various sands with different relative densities, the corresponding fitting coefficients, A_1, was around −1, and B_1 was around 1. When using unified $A_1 = -1$ and $B_1 = 1$, the re-calculated R^2 was 0.967. Therefore, the variation of $G_{max,N}/G_{max,0}$ versus pore pressure ratio for different types of sands with different relative densities can all be written as follows:

$$G_{max,N} = G_{max,0} \cdot (1 - U_N) \tag{3}$$

Equation (3) expresses the variation of $G_{max,N}/G_{max,0}$ versus the pore pressure ratio. It can also be referred to as the calculation equation for the $G_{max,N}/G_{max,0}$ versus pore pressure increase.

3.3 Cyclic $\tau_{ult,N}$ Under Increasing Pore Pressure and Its Fitted Equation

The cyclic ultimate shear stress $\tau_{ult,N}$ obtained from experiments is normalized to achieve the relationship between the cyclic ultimate shear stress ratio, $\tau_{ult,N}/\tau_{ult,0}$, and the pore pressure ratio. Figure 3 reveals that the experimental points are approximate to a quadratic curve. Thus, the relationship between $\tau_{ult,N}/\tau_{ult,0}$ and the pore water pressure under each stress cycle can be written as follows:

$$\tau_{ult,N} / \tau_{ult,0} = aU_N^2 = bU_N + c \tag{4}$$

where a, b and c are coefficients to be determined. The fitting parameters and R^2 determined by Equation (4) are provided in Table 3.

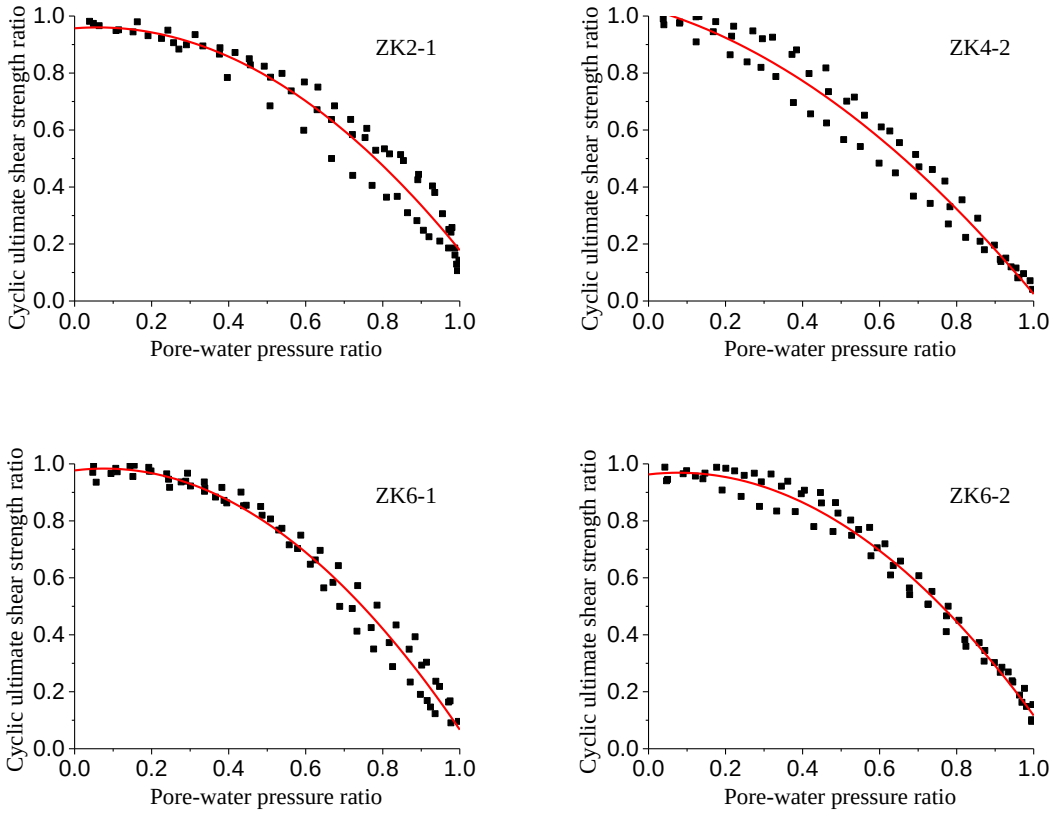

Fig. 3 Quadratic regressions of cyclic ultimate shear strength ratios with respect to pore-water pressure ratios

Figure 3 indicates that the cyclic $\tau_{ult,N}$ decreases with the increase of the pore pressure ratio, this response varies according to relative density. The variation of $\tau_{ult,N}/\tau_{ult,0}$ with pore pressure ratio for Yingkou sand was described by a convex hyperbolic curve. This observation is reflected by the different sizes of regression parameters (shown in Table 3). Therefore, the relative density of sand has an impact on the variation model and specific forms of the cyclic $\tau_{ult,N}/\tau_{ult,0}$ changing with pore pressure ratio.

Table 3 Regression parameters of variation curves for cyclic ultimate shear stress versus pore pressure ratio

No.	*a*	*b*	*c*	Correlation coefficient R^2
ZK2-1	−0.88	0.10	0.96	0.951
ZK4-2	−0.61	−0.39	1.03	0.968
ZK6-1	−1.08	0.17	0.98	0.977
ZK6-2	−1.00	0.15	0.96	0.983

4. Conclusions

Focusing on saturated sandy soils with different relative densities, liquefaction testing under the application of dynamic stress with unified equal consolidation and different equal amplitudes with a new type of high-precision dynamic three-axis instrument are carried out. The fitted curves to describe the cyclic $G_{max,N}$ and cyclic $\tau_{ult,N}$ under increasing pore pressure are obtained, and proposed equations with different precisions for the calculation of these parameters. The major conclusions are presented as follows:

(1) The increase of pore pressure has a major impact on the cyclic $G_{max,N}$ and cyclic ultimate shear stress of sandy soil. With the increase of pore pressure ratio, the cyclic $G_{max,N}$ and cyclic ultimate shear stress decrease.

(2) Not only the model to describe the variation of the cyclic $G_{max,N}$ with pore pressure ratio, but also the calculation equations of the cyclic $G_{max,N}$ under pore pressure increase can be written as a unified linear expression. This expression independent of the relative density of sand, and the corresponding pore pressure ratio is equal to the relative reduction of the cyclic $G_{max,N}$.

(3) The models to describe the variation of the cyclic $\tau_{ult,N}$ versus pore pressure ratio were not consistent for several sandy soils with different relative densities, and they exhibited as a hyperbolic curve.

This research carried out liquefaction testing using equal-amplitude loading under unified equal consolidation. For the application of irregular loading and the condition of non-unified equal consolidation, the behaviors of the maximum shear modulus and $\tau_{ult,N}$ for sandy soils require more specific investigation.

4. Acknowledgements

The research is supported jointly by the Scientific Research Fund of Institute of Engineering Mechanics, China earthquake Administration (2018A01), the National Key Technology Support Program (2015BAK17B01) and the Heilongjiang and National Natural Science Foundation of China (ZD2019E009, 51278472, 1272357).

5. References

[1] Kondner R. L. (1963): Hyperbolic stress strain response: cohesive soils. *Journal of the Soil Mechanics & Foundations Division, ASCE*, **89**(1), 115-143.

[2] Hardin, B. O, Drnevich, V. P(1972): Shear Modulus and Damping in Soils. *Journal of Geotechnical Engineering Division, ASCE*, **98**(6), 603-624.

[3] Matasovic N., Vucetic M. (1992): Cyclic characterization of liquefiable sands. *Journal of Geotechnical Engineering*. **119**(11), 1805-1822.

[4] Dobry R., Ladd R., Yokel F., et al(1982): Prediction of pore water pressure buildup and liquefaction of sands during earthquakes by the cyclic strain method. *National Bureau of Standards Building Science Series* 138.

